Earthline Journal of Mathematical Sciences
E-ISSN: 2581-8147
Volume 15, Number 5, 2025, Pages 723-748
https://doi.org/10.34198/ejms.15525.723748

Mathematical Model and Analysis of Toxicant Effect on Human Health in Fuzzy Environment

Kenneth Ojotogba Achema

Joseph Sarwuan Tarka University, Makurdi, Benue State, Nigeria
e-mail: achema.kenneth@uam.edu.ng

Abstract

A nonlinear mathematical model is proposed and analyzed to examine the impact of a toxicant effect on human health in fuzzy environment, specifically its detrimental effects on the reproductive health of a subclass within the species. By applying stability theory, it is demonstrated that the overall species population stabilizes at an equilibrium level. Additionally, findings indicate that as the toxicant emission rate increases, the population density of the subclass severely affected by the toxicant—rendered incapable of reproduction—also rises.

1 Introduction

Homo sapiens have always been exposed to various environmental toxins, including particles, smoke from fire usage, thermal processing food-related toxicants, fecal aerosols, and pathogens transmitted by domestic animals, especially in high population densities seen in post-Neolithic societies. Even today, some human populations have developed genetic adaptations to their environments, resulting in higher frequencies of protective variants against harmful substances. For example, South American populations have shown genetic adaptations to arsenic (As), a naturally occurring toxic chemical [2].

With the advent of the Industrial Revolution and technological progress, humans began to face contaminants never encountered in nature before, such as industrial byproducts, cigarette smoke, and air pollution [1,3]. These changes are too recent to have triggered genetic adaptation, and modern clinical practices and urban environments have further weakened the effects of selective pressures [4]. However, epigenetic processes are believed to be crucial molecular mechanisms for medium-term adaptation, enabling the body to respond to early exposure to new environmental factors [5–7], possibly creating an epigenetic signature of exposure.

Received: April 5, 2025; Accepted: May 28, 2025; Published: June 16, 2025
2020 Mathematics Subject Classification: 92D30, 93D05.
Keywords and phrases: toxicant, mathematical model, fuzzy, DNA methylation.

Epigenetic mechanisms influence gene expression without altering the DNA sequence itself [8]. Among these, DNA methylation is one of the most studied. In mammals, DNA methylation occurs at CpG sites, involving the addition of a methyl group (-CH3) to the 5' position of cytosine, resulting in 5-methylcytosine (5mC). DNA methyltransferases (DNMTs) catalyze this process using S-adenosyl-l-methionine (SAM) as a methyl donor. DNMTs include those responsible for de novo methylation (DNMT3A and DNMT3B) and the maintenance of pre-existing methylation patterns during cell division (DNMT1) [9].

Exposure to toxic agents can drive natural variation and shape human biodiversity. Two primary sources of biological variability related to toxicants exposure are genetic variability, observed in human populations as a result of long-term adaptation, and epigenetic variability, such as altered DNA methylation profiles, which can be seen both at the individual and population levels and may influence mutation rates (medium-term adaptation).

Human populations have exhibited genetic variability due to adaptive responses to various environmental factors throughout their evolution. For instance, the aridification of North Africa 7-11 million years ago led to the formation of deserts and savannas, resulting in environmental changes that exposed early hominids to new types of aerosols. Innate immunity receptors, such as the Macrophage Receptor with Collagenous Structure (MARCO), played a central role in responding to these exposures. Certain genetic changes, such as substitutions in MARCO, have been positively selected, altering its ability to bind and phagocytose inhaled substances [1].

Researchers suggest that changes in aerosol exposure may have increased the need for more efficient innate immunity receptors, prompting genetic changes over time. The discovery of fire further exposed early humans to new environmental stress, including the smoke from burning wood, which contains toxic and carcinogenic substances like polycyclic aromatic hydrocarbons (PAHs) has been established [1,16,17].

An example of genetic adaptation to toxicants can be seen in South American populations exposed to arsenic (As), a naturally occurring toxic element. Indigenous communities in certain regions have developed higher frequencies of protective genetic variants, enabling them to better tolerate arsenic exposure through mechanisms like increased excretion of arsenic via methylation [2,18,19].

The phenotypic variability observed between individuals and populations cannot be solely explained by genetic differences. Epigenetic mechanisms, such as DNA methylation, play a crucial role in regulating gene expression and can explain some of the differences between genetically identical individuals, like monozygotic twins, who exhibit differing DNA methylation patterns [20]. Thus, the epigenome, particularly DNA methylation, is key to phenotypic diversity between populations. While some studies question the role of DNA methylation in human evolution, evidence shows that DNA methylation dynamics can affect mutation rates, particularly at methylated CpG sites [21,22]. Recent research also suggests that endocrine disruptors, while not directly causing genetic mutations, can influence genetic instability through

epigenetic changes, thereby promoting mutation and variation [23,24].

A recent study on the Faroe Islands examined the effects of various chemicals in food and fish on DNA methylation in cord blood. The study found that exposure to pollutants like Methyl mercury, PCBs, and others was linked to DNA methylation changes, with some sex-specific differences observed in the DNA methylation patterns of males and females [25]. Other studies on air pollution also showed that long-term exposure to pollutants like PM10 and PM2.5 negatively impacted sperm motility, DNA methylation, and reproductive fitness in both mice and humans [26–28].

Although male infertility is prevalent, female infertility appears to be more widespread. Oocytes in females remain demethylated until puberty, making childhood a critical period for environmental exposure. Studies on chemicals like Methoxychlor, an endocrine disruptor, have shown that exposure can lead to DNA methylation changes in specific genes, such as those related to estrogen receptors in the ovaries, potentially affecting female reproductive health [29].

Considering the importance of epigenetic mechanisms, particularly DNA methylation, in responding to new environmental factors, this study aims to examine recent literature (primarily on humans) to explore the impact of major industrial-era contaminants on human evolution with the aid of mathematical model. It focuses on the effects of toxicants on DNA methylation and their evolutionary implications, including reproductive fitness, survival, biodiversity, mutation rates.

The organisation of this paper is as follows. The model is formulated in Section 2. The analyses of the formulated model and its numerical simulation are carried out in Section 3, while the results of the model analyses and simulations are discussed in Section 4. The main results and discussion from this study are summarized in Section 5 while the study conclusion is carried out in Section 6.

2 Model Formulation

2.1 Assumptions of the model equations

For proper understanding and formulation of system of equations in this study, we present the following assumptions:

(A_1) It is assumed that human environment is affected by different chemicals known as toxicant.

(A_2) It is also assumed that toxicant has severe effect on human health after exposure.

(A_3) Human population carrying capacity (K) is a function of toxicant concentration.

(A_4) Human population are affected by the environmental toxicant through food chain, air pollution, and contaminated water.

2.2 Model variables and parameters

Table 1: Description of the model variables and parameters

Variable	Interpretation
$P(t)$	Human population at time t
$P_D(t)$	Deformed human population at time t
$C(t)$	Concentration of toxicant at time t
$U(t)$	Uptake concentration of toxicant at time t
Parameter	Interpretation
r	Intrinsic growth rate of human population
K	Carrying capacity of human population
Q	Influx of toxicant concentration
δ	Natural depletion rate of toxicant concentration
γ	Quantity of concentration of toxicant uptake by human population
v	Rate at which dead human decay added back to toxicant concentration
ϕ	Quantity of excreted toxicant concentration uptake by human population
d	Death rate of the deformed human population
λ	Rate at which some persons that are affected by toxicant become deformed
b	Birth rate of the population

2.3 Descriptions of the model equations

The model equations is subdivided into four (4) ecological compartments namely health human population (P), deformed human population (P_D), concentration of toxicant in human environment (C), and uptake(inhaled, through food chain) of toxicant concentration (U). The human population is logistically modelled. The concentration of toxicant (C) and the uptake concentration of toxicant (U) are modelled by the law of chemical and biological behaviours respectively.

2.4 Model equations

Keeping track of the above assumptions, variables, parameters descriptions, and the model equations description, the formulated model equations are given by

$$\frac{dP}{dt} = rP - \frac{rP^2}{K(C)} - (\xi + b)P_D \tag{1}$$

$$\frac{dP_D}{dt} = \lambda P'U - \frac{rP_DP}{K(C)} - (\xi + d)P_D \tag{2}$$

$$\frac{dC}{dt} = QP - \delta C - \gamma CP + \theta vPU \tag{3}$$

$$\frac{dU}{dt} = \gamma CP - \phi U - vPU \tag{4}$$

with initial data: $P(0) \geq 0, P_D(0) \geq 0, C(0) \geq 0, U(0) \geq cP(0), c > 0, 0 \leq \pi \leq 1$. and $P' = P - P_D$. The initial conditions of this model are completely possible if and only if there is a deliberate poisoning of human population sources of food or use of chemical weapon during war. In a natural setting, the human population will continue to exist.

The fuzzy representation of the model equations (1 - 4) can be expressed as follows:

$$\frac{dP}{dt} = rP - \frac{rP^2}{K(C)} - (\xi + b)P_D \tag{5}$$

$$\frac{dP_D}{dt} = \lambda P'U - \frac{rP_DP}{K(C)} - (\xi + d)P_D \tag{6}$$

$$\frac{dC}{dt} = Q(\omega)P - \delta C - \gamma(\omega)CP + \theta vPU \tag{7}$$

$$\frac{dU}{dt} = \gamma(\omega)CP - \phi U - vPU \tag{8}$$

It is assumed that the influx of toxicant into human environment is at per capita rate denoted by $Q(\omega)$ and the fraction of uptake concentration of toxicant by the human, $\gamma(\omega)$, are represented as fuzzy numbers, contigent upon the predator's concentration uptake. The variable $Q(\omega)$ is defined by Barros et al. [32] as

$$Q(\omega) = \begin{cases} 0 & \omega < \omega_{min}, \\ \frac{\omega - \omega_{min}}{\omega_M - \omega_{min}}, & \omega_{min} \leq \omega \leq \omega_M \\ 1, & \omega_M < \omega, \end{cases}$$

The $Q(\omega)$ attains its peak when ω is its maximum value, and it becomes immaterial when ω is at its minimum. ω_{min} represents the minimum toxicant concentration influx required for human's deformity, and the concentration of toxicant is at its highest when $\omega = \omega_M$, attaining or approaching a value of 1. Similarly, $\gamma(\omega)$ is defined as (Verna et al. [34]).

$$\gamma(\omega) = \left\{ \frac{Q_0 - 1}{\omega_M}\omega + 1, 0 \leq \omega \leq \omega_M \right.$$

where $Q_0 > 0$ is the minimum concentration of the toxicant influx rate.

2.5 Equilibrium analysis

The analysed model has two toxicant-free equilibrium points and two toxicant-present equilibrium points.

Case 1. If $\omega \leq \omega_{min}$ and $\gamma(\omega) > 0$ then $Q(\omega) = 0$ and we get the following two TFE points:

$$E_0 = (0, 0, 0, 0) \text{ and } E_1 = (K_0, 0, 0, 0).$$

In this case, we will ignore the E_0 equilibrium and stick to E_1 equilibrium since the analysis of E_0 equilibrium is trivial. However, the E_0 equilibrium is completely possible if and only if there is a deliberate poisoning of human population sources of food or use of chemical weapon during war. In a natural setting, the human population will continue to exist.

Case 2. If $\omega_{min} \leq \omega \leq \omega_M$ and $\gamma(\omega) > 0$ then $Q(\omega) = \frac{\omega - \omega_{min}}{\omega_M - \omega_{min}}$ and we get

$$E^* = (P^*, P_D^*, C^*, U^*)$$

where

$$P^* = \frac{K(C)(\lambda + \xi + d)P_D^*}{K(C)\lambda - rP_D^*}, P_D^* = \frac{K(C)rP^* - rP^{*2}}{K(C)(\xi + b)}, C^* = \frac{(Q(\omega) + \theta v U^*)P^*}{\delta + \gamma(\omega)P^*}, U^* = \frac{\gamma(\omega)C^*P^*}{\phi + vP^*}.$$

Case 3. If $\omega_M < \omega$ and $\gamma(\omega) > 0$ then $Q(\omega) = 1$ and we get

$$E^{**} = (P^{**}, P_D^{**}, C^{**}, U^{**})$$

where

$$P^{**} = \frac{K(C)(\lambda + \xi + d)P_D^{**}}{K(C)\lambda - rP_D^{**}}, P_D^{**} = \frac{K(C)rP^{**} - rP^{**2}}{K(C)(\xi + b)}, C^{**} = \frac{(1 + \theta v U^{**})P^{**}}{\delta + \gamma(\omega)P^{**}}, U^{**} = \frac{\gamma(\omega)C^{**}P^{**}}{\phi + vP^{**}}.$$

The equilibrium points $E*$ and E^{**} represent situations where toxicant concentrations persist in human's environment exceeds the minimum threshold necessary for its deformity, resulting in the oscillation of the human population.

Stability analysis

To carry out the model stability, we shall rewrite Equations (5 - 8) as follows.

$$B_1 = rP - \frac{rP^2}{K(C)} - (\xi + b)P_D \tag{9}$$

$$B_2 = \lambda P'U - \frac{rP_DP}{K(C)} - (\xi + d)P_D \tag{10}$$

$$B_3 = Q(\omega)P - \delta C - \gamma(\omega)CP + \theta vPU \tag{11}$$

$$B_4 = \gamma(\omega)CP - \phi U - vPU \tag{12}$$

The Jacobian matrix of the system of Equations (9) - (12) can be represented by

$$J_1 = \begin{pmatrix} \frac{\partial B_1}{\partial P} & \frac{\partial B_1}{\partial P_D} & \frac{\partial B_1}{\partial C} & \frac{\partial B_1}{\partial U} \\ \frac{\partial B_2}{\partial P} & \frac{\partial B_2}{\partial P_D} & \frac{\partial B_2}{\partial C} & \frac{\partial B_2}{\partial U} \\ \frac{\partial B_3}{\partial P} & \frac{\partial B_3}{\partial P_D} & \frac{\partial B_3}{\partial C} & \frac{\partial B_3}{\partial U} \\ \frac{\partial B_4}{\partial P} & \frac{\partial B_4}{\partial P_D} & \frac{\partial B_4}{\partial C} & \frac{\partial B_4}{\partial U} \end{pmatrix}$$

$$\therefore J_1 = \begin{pmatrix} r - \frac{2rP}{K(C)} & -(\xi + b) & 0 & 0 \\ \lambda U - \frac{rP_D}{K(C)} & -\lambda U - \frac{rP}{K(C)} & 0 & \lambda(P - P_D) \\ Q(\omega) - \gamma(\omega)C + \theta vU & 0 & -\delta - \gamma(\omega)P & \theta vP \\ \gamma(\omega)C - vU & 0 & \gamma(\omega)P & -\theta - vP \end{pmatrix}$$

$$\therefore J_1(E_1) = \begin{pmatrix} -r & -(\xi + b) & 0 & 0 \\ 0 & -r & 0 & \lambda K_0 \\ Q(\omega) & 0 & -\delta - \gamma(\omega)K_0 & \theta vK_0 \\ 0 & 0 & \gamma(\omega)K_0 & -\theta - vK_0 \end{pmatrix}$$

System Eqs. $(1) - (4)$ is locally asymptotic stable when the absolute eigenvalues of the Jacobian matrix in Eq.(15) have negative real parts.

3 Numerical Investigation

3.1 Forward Euler Scheme

The Forward Euler scheme is a well-known explicit first-order numerical approach for solving ordinary differential equations. It provides a fast estimation of the behaviour of solution over time computational efficient.

$$P^{n+1} = P^n + h\big[rP^n - \frac{rP^{n2}}{K(C)} - (\xi + b)P_D^n\big] \tag{13}$$

$$P_D^{n+1} = P_D^n + h\big[\lambda(P^2 - P_D^n)U^n - \frac{rP^{n2}}{K(C)} - (\xi + b)P_D^n\big] \tag{14}$$

$$C^{n+1} = C^n + h\big[Q(\omega)P^n - \delta C^n - \gamma(\omega)C^nP^n + \theta vP^nU^n\big] \tag{15}$$

$$U^{n+1} = U^n + h\big[\gamma(\omega)C^nP^n - \phi U^n - vP^nU^n\big] \tag{16}$$

Case 1. If $\omega < \omega_{min}$ and $\gamma(\omega) > 0$ then $Q(\omega) = 0$ and

$$P^{n+1} = P^n + h\big[rP^n - \frac{rP^{n2}}{K(C)} - (\xi - b)P_D^n\big] \tag{17}$$

$$P_D^{n+1} = P_D^n + h\big[\lambda(P^2 - P_D^n)U^n - \frac{rP_D^nP^n}{K(C)} - (\xi + b)P_D^n\big] \tag{18}$$

$$C^{n+1} = C^n - h\big[\delta C^n + \gamma(\omega)C^nP^n - \theta vP^nU^n\big] \tag{19}$$

$$U^{n+1} = U^n + h\big[\gamma(\omega)C^nP^n - \phi U^n - vP^nU^n\big] \tag{20}$$

Case 2. If $\omega_{min} \leq \omega \leq \omega_M$ and $\gamma(\omega) > 0$ then $Q(\omega) = \frac{\omega - \omega_{min}}{\omega_M - \omega_{min}}$ and the Euler scheme becomes

$$P^{n+1} = P^n + h\big[rP^n - \frac{rP^{n2}}{K(C)} - (\xi + b)P_D^n\big] \tag{21}$$

$$P_D^{n+1} = P_D^n + h\big[\lambda(P^2 - P_D^n)U^n - \frac{rP^{n2}}{K(C)} - (\xi + b)P_D^n\big] \tag{22}$$

$$C^{n+1} = C^n + h\big[Q(\omega)P^n - \delta C^n - \gamma(\omega)C^nP^n + \theta vP^nU^n\big] \tag{23}$$

$$U^{n+1} = U^n + h\big[\gamma(\omega)C^nP^n - \phi U^n - vP^nU^n\big] \tag{24}$$

Case 3. If $\omega_M < \omega$ and $\gamma(\omega) > 0$ then $Q(\omega) = 1$ and

$$P^{n+1} = P^n + h\big[rP^n - \frac{rP^{n2}}{K(C)} - (\xi + b)P_D^n\big] \tag{25}$$

$$P_D^{n+1} = P_D^n + h\big[\lambda(P^2 - P_D^n)U^n - \frac{rP^{n2}}{K(C)} - (\xi + b)P_D^n\big] \tag{26}$$

$$C^{n+1} = C^n + h\big[P^n - \delta C^n - \gamma(\omega)C^nP^n + \theta vP^nU^n\big] \tag{27}$$

$$U^{n+1} = U^n + h\big[\gamma(\omega)C^nP^n - \phi U^n - vP^nU^n\big] \tag{28}$$

3.2 Non-standard finite difference (NSFD)scheme

The scheme, NSFD is a class of numerical methods for approximating solutions of differential equations. This method is not the same as the traditional finite difference methods in their approach to discretizing the domain and its derivatives approximation. The numerical model, NSFD is formulated based on Mickens [33] NSFD theory.

$$P^{n+1} = \frac{P^n + hK(C)(\lambda + \xi + d)P_D}{1 + h(K(C)\lambda - rP_D)} \tag{29}$$

$$P^{n+1} = \frac{P_D^n + h[K(C)rP - rP^2]}{1 + hK(C)(\xi + b)} \tag{30}$$

$$C^{n+1} = \frac{C^n + h(Q(\omega) + \phi vU)}{1 + h(\delta + \gamma(\omega)P)} \tag{31}$$

$$U^{n+1} = \frac{U^n + h\gamma(\omega)CP}{1 + h(\phi + vP)} \tag{32}$$

Case 1. If $\omega < \omega_{min}$ and $\gamma(\omega) > 0$ then $Q(\omega) = 0$ and the NSFD scheme becomes

$$P^{n+1} = \frac{P^n + hK(C)(\lambda + \xi + d)P_D}{1 + h(K(C)\lambda - rP_D)} \tag{33}$$

$$P^{n+1} = \frac{P_D^n + h[K(C)rP - rP^2]}{1 + hK(C)(\xi + b)} \tag{34}$$

$$C^{n+1} = \frac{C^n + h\phi vUP}{1 + h(\delta + \gamma(\omega)P)} \tag{35}$$

$$U^{n+1} = \frac{U^n + h\gamma(\omega)CP}{1 + h(\phi + vP)} \tag{36}$$

Case 2. If $\omega_{min} \leq \omega \leq omega_M$ and $\gamma(\omega) > 0$ then $Q(\omega) = \frac{\omega - \omega_{min}}{\omega_M - \omega_{min}}$ and the NSFD scheme becomes

$$P^{n+1} = \frac{P^n + hK(C)(\lambda + \xi + d)P_D}{1 + h(K(C)\lambda - rP_D)} \tag{37}$$

$$P^{n+1} = \frac{P_D^n + h[K(C)rP - rP^2]}{1 + hK(C)(\xi + b)} \tag{38}$$

$$C^{n+1} = \frac{C^n + h(Q(\omega) + \phi vU)}{1 + h(\delta + \gamma(\omega)P)} \tag{39}$$

$$U^{n+1} = \frac{U^n + h\gamma(\omega)CP}{1 + h(\phi + vP)} \tag{40}$$

Case 3. If $\omega_M < \omega$ and $\gamma(\omega) > 0$ then $Q(\omega) = 1$ and the scheme becomes

$$P^{n+1} = \frac{P^n + hK(C)(\lambda + \xi + d)P_D}{1 + h(K(C)\lambda - rP_D)} \tag{41}$$

$$P^{n+1} = \frac{P_D^n + h[K(C)rP - rP^2]}{1 + hK(C)(\xi + b)} \tag{42}$$

$$C^{n+1} = \frac{C^n + h(Q(1 + \phi vU)}{1 + h(\delta + \gamma(\omega)P)} \tag{43}$$

$$U^{n+1} = \frac{U^n + h\gamma(\omega)CP}{1 + h(\phi + vP)} \tag{44}$$

3.3 Consistency analysis

In this section, we shall check the consistency of the NSFD scheme of the Eqs. $(29 - 32)$ as follows. We start by considering Eq. (29), and we get

$$P^{n+1}[1 + h(K(C)\lambda - rP_D)] = P^n + hK(C)(\lambda + \xi + d)P_D \tag{45}$$

Taking into account the Taylor's series expansion for P^{n+1}, we obtain

$$P^{n+1} = P^n + h\frac{dP}{dt} + \frac{h^2}{2!}\frac{dP}{dt} + \frac{h^3}{3!}\frac{dP}{dt} + ... \tag{46}$$

Substituting Eq.(46) in Eq.(45), we have

$$\left(P^n + h\frac{dP}{dt} + \frac{h^2}{2!}\frac{dP}{dt} + \frac{h^3}{3!}\frac{dP}{dt} + ...\right)\left[1 + h(K(C)\lambda - rP_D)\right] = P^n + hK(C)(\lambda + \xi + d)P_D \tag{47}$$

As $h \to 0$, we have

$$\frac{dP}{dt} + (K(C)\lambda - rP_D)P^n = K(C)(\lambda + \xi + d)P_D \tag{48}$$

or

$$\frac{dP}{dt} = K(C)(\lambda + \xi + d)P_D - (K(C)\lambda - rP_D)P^n \tag{49}$$

From Eq. (30), we get

$$P_D^{n+1}[1 + hK(C)(\xi + b)] = P_D^n + h[K(C)rP - rP^2] \tag{50}$$

Also, taking into consideration the Taylor's series expansion for P_D^{n+1}, we get

$$P_D^{n+1} = P_D^n + h\frac{dP_D}{dt} + \frac{h^2}{2!}\frac{dP_D}{dt} + \frac{h^3}{3!}\frac{dP_D}{dt} + ... \tag{51}$$

Substituting Eq. (51) in Eq. (50), we have

$$\left(P_D^n + h\frac{dP_D}{dt} + \frac{h^2}{2!}\frac{dP_D}{dt} + \frac{h^3}{3!}\frac{dP_D}{dt} + ...\right)\left[1 + hK(C)(\xi + b)\right] = P_D^n + h\left[K(C)rP - rP^2\right] \tag{52}$$

As $h \to 0$, we have

$$K(C)(\xi + b)P_D^n + \frac{dP_D}{dt} = K(C)rP - rP^2 \tag{53}$$

or

$$\frac{dP_D}{dt} = (K(C) - P)rP - K(C)(\xi + b)P_D^n \tag{54}$$

From Eq. (31), we have

$$C^{n+1}\big[1 + h(\delta + \gamma(\omega)P)\big] = C^n + h(Q(\omega) + \phi vU)P \tag{55}$$

More so, taking into account the Taylor's series expansion for C^{n+1}, we have

$$C^{n+1} = C^n + h\frac{dC}{dt} + \frac{h^2}{2!}\frac{dC}{dt} + \frac{h^3}{3!}\frac{dC}{dt} + ... \tag{56}$$

Substituting Eq. (56) in Eq. (55), we obtain

$$\Big(C^n + h\frac{dC}{dt} + \frac{h^2}{2!}\frac{dC}{dt} + \frac{h^3}{3!}\frac{dC}{dt} + ...\Big)\big[1 + h(\delta + \gamma(\omega)P)\big] = C^n + h(Q(\omega) + \phi vU)P \tag{57}$$

As $h \to 0$, we have

$$\frac{dC}{dt} + \delta + \gamma(\omega)P = (Q(\omega) + \phi vU)P \tag{58}$$

or

$$\frac{dC}{dt} = \big(Q(\omega) + \phi vU\big)P - (\delta + \gamma(\omega)P) \tag{59}$$

Finally, from Eq. (32), we get

$$U^{n+1}[1 + h(\phi + vP)] = U^n + h\gamma(\omega)CP \tag{60}$$

Taking into consideration the Taylor's expansion for U^{n+1}, we have

$$U^{n+1} = U^n + h\frac{dU}{dt} + \frac{h^2}{2!}\frac{dU}{dt} + \frac{h^3}{3!}\frac{dU}{dt} + ... \tag{61}$$

Substituting Eq. (61) in Eq. (60), we obtain

$$\Big(U^n + h\frac{dU}{dt} + \frac{h^2}{2!}\frac{dU}{dt} + \frac{h^3}{3!}\frac{dU}{dt} + ...\Big)\big[1 + h(\phi + vP)\big] = U^n + h\gamma(\omega)CP \tag{62}$$

As $h \to 0$, we have

$$\frac{dU}{dt} + \phi + vP = \gamma(\omega)PC \tag{63}$$

or

$$\frac{dU}{dt} = \gamma(\omega)CP - (\phi + vP) \tag{64}$$

Thus, we can categorically say that the NSFD scheme model exhibits first-order consistency.

3.4 Stability of the non-standard finite difference (NSFD) scheme

To carry out the stability analysis, we shall rewrite the Eqs. $(29-32)$ as follows:

$$P^{n+1} = C_1 = \frac{P^n + hK(C)(\lambda + \xi + d)P_D}{1 + h(K(C)\lambda - rP_D)} \tag{65}$$

$$P^{n+1} = C_2 = \frac{P_D^n + h[K(C)rP - rP^2]}{1 + hK(C)(\xi + b)} \tag{66}$$

$$C^{n+1} = C_3 = \frac{C^n + h(Q(\omega) + \phi vU)}{1 + h(\delta + \gamma(\omega)P)} \tag{67}$$

$$U^{n+1} = C_4 = \frac{U^n + h\gamma(\omega)CP}{1 + h(\phi + vP)} \tag{68}$$

4 Numerical Illustration

In order to appreciate the analytical results, numerical simulation of the model equations (1) is presented by using the following set of parameter values (see Table 2).

Table 2: Parameter values of the model equations

Parameter	Value	Source
r	0.8	(Kumar [31])
K	10 - 1000	Varied
Q	0.001 - 0.009	Varied
δ	0.025	(Kumar [31])
γ	0.001	Assumed
v	0.001	(Achema et al. [30])
ϕ	0.01	(Achema et al. [30])
d	0.0001	(Kumar [31])
λ	0.3	Assumed
b	0.05	Assumed

5 Results and Discussion

The analysis reveals that when the toxicant emission rate Q reaches a critical threshold ($Q = 0.005$), the system loses stability, leading to periodic oscillations. As the emission rate increases, the total population

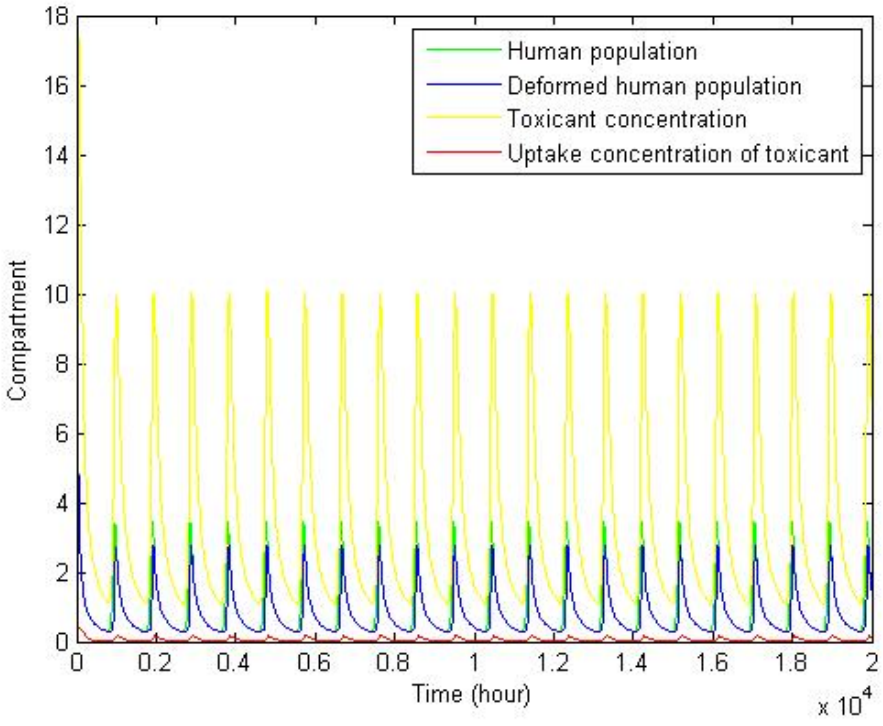
Human population
Deformed human population
Toxicant concentration
Uptake concentration of toxicant
Compartment
Time (hour)
x 10^4
0
2
4
6
8
10
12
14
16
18
0
0.2
0.4
0.6
0.8
1
1.2
1.4
1.6
1.8
2

Figure 1:

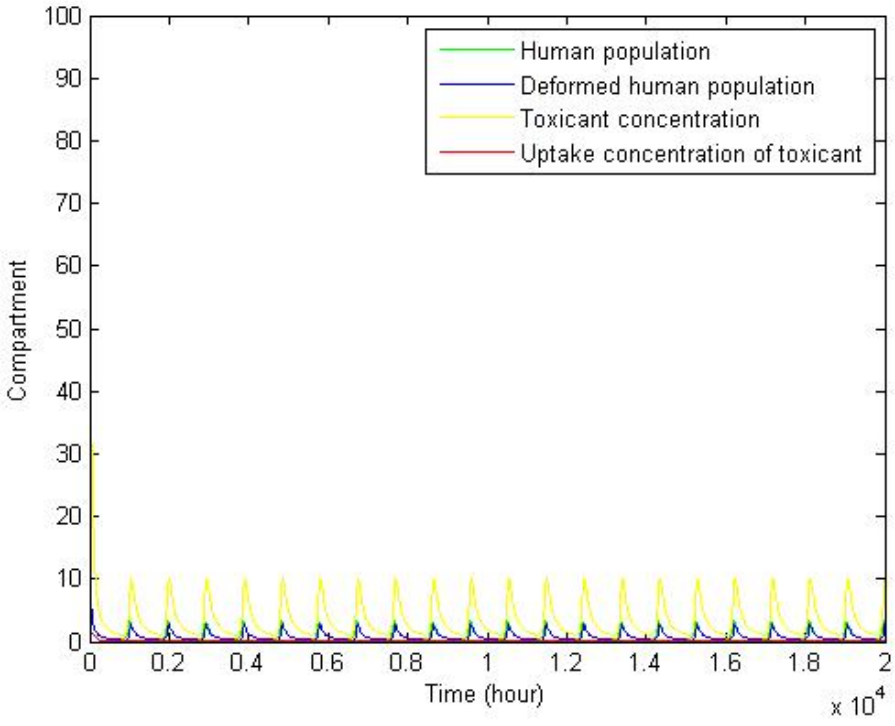
Human population
Deformed human population
Toxicant concentration
Uptake concentration of toxicant
Compartment
Time (hour)
x 10^4
0
10
20
30
40
50
60
70
80
90
100
0.2
0.4
0.6
0.8
1
1.2
1.4
1.6
1.8
2

Figure 2:

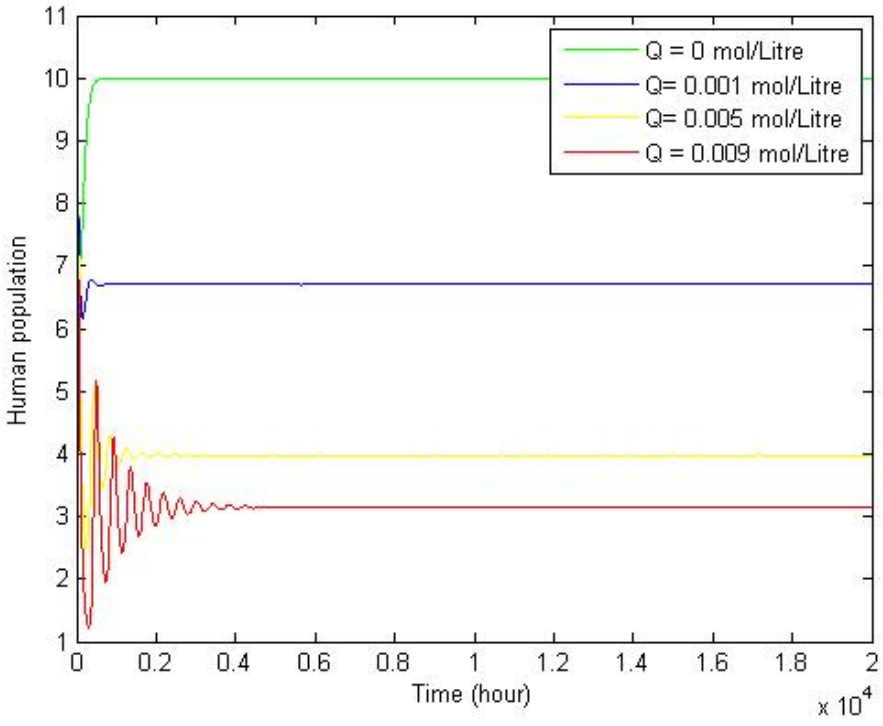
Q = 0 mol/Litre
Q= 0.001 mol/Litre
Q= 0.005 mol/Litre
Q = 0.009 mol/Litre
Human population
Time (hour)
x 10^4
11
10
9
8
7
6
5
4
3
2
1
0
0.2
0.4
0.6
0.8
1
1.2
1.4
1.6
1.8
2

Figure 3:

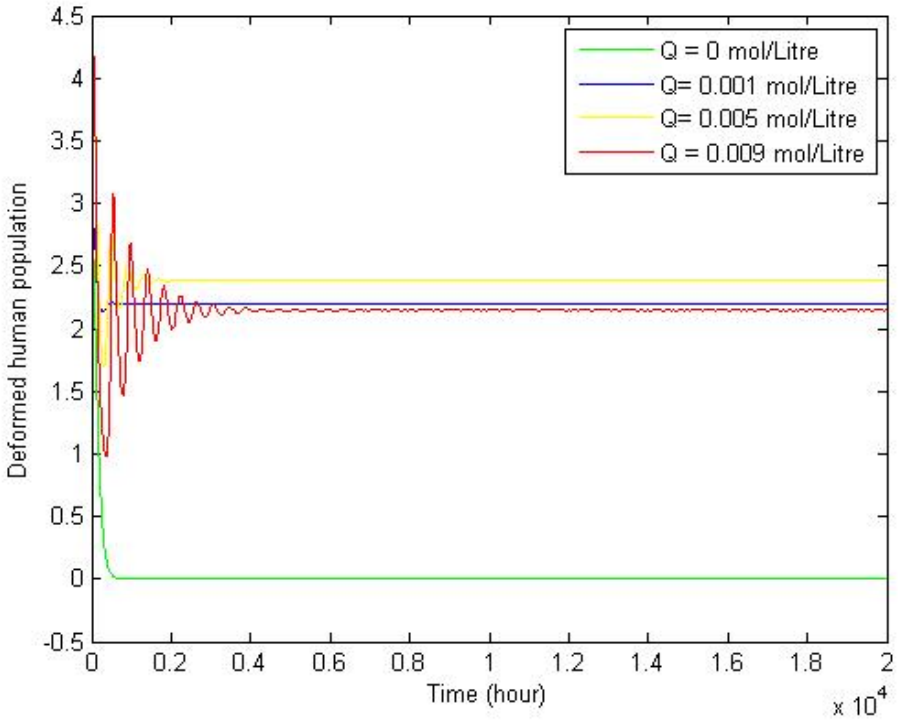
Q = 0 mol/Litre
Q= 0.001 mol/Litre
Q= 0.005 mol/Litre
Q = 0.009 mol/Litre
Deformed human population
Time (hour)
x 10^4
4.5
4
3.5
3
2.5
2
1.5
1
0.5
0
-0.5
0
0.2
0.4
0.6
0.8
1
1.2
1.4
1.6
1.8
2

Figure 4:

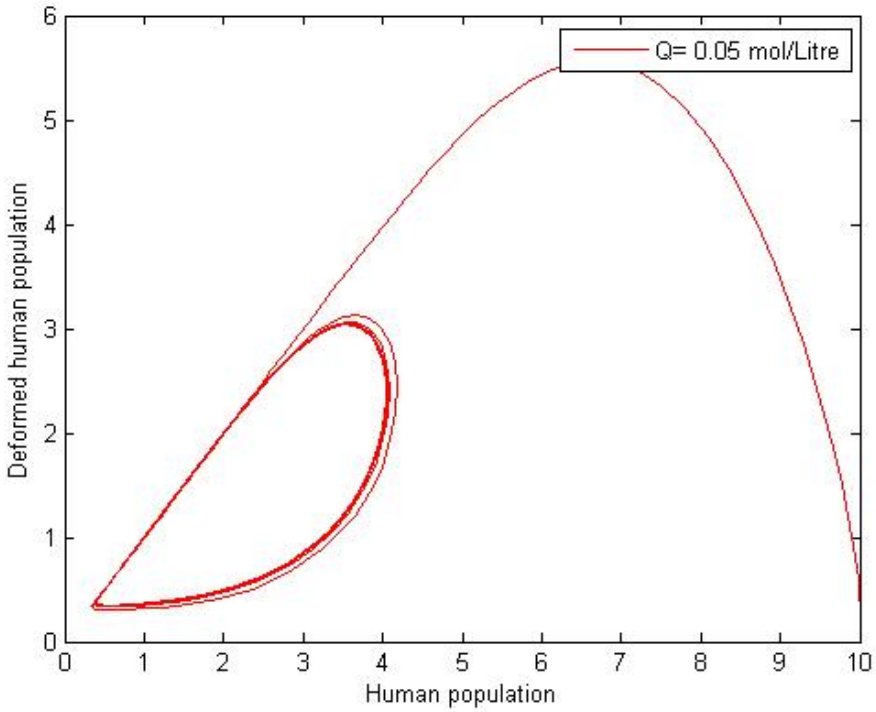
Q= 0.05 mol/Litre
Deformed human population
Human population
0
1
2
3
4
5
6
7
8
9
10

Figure 5:

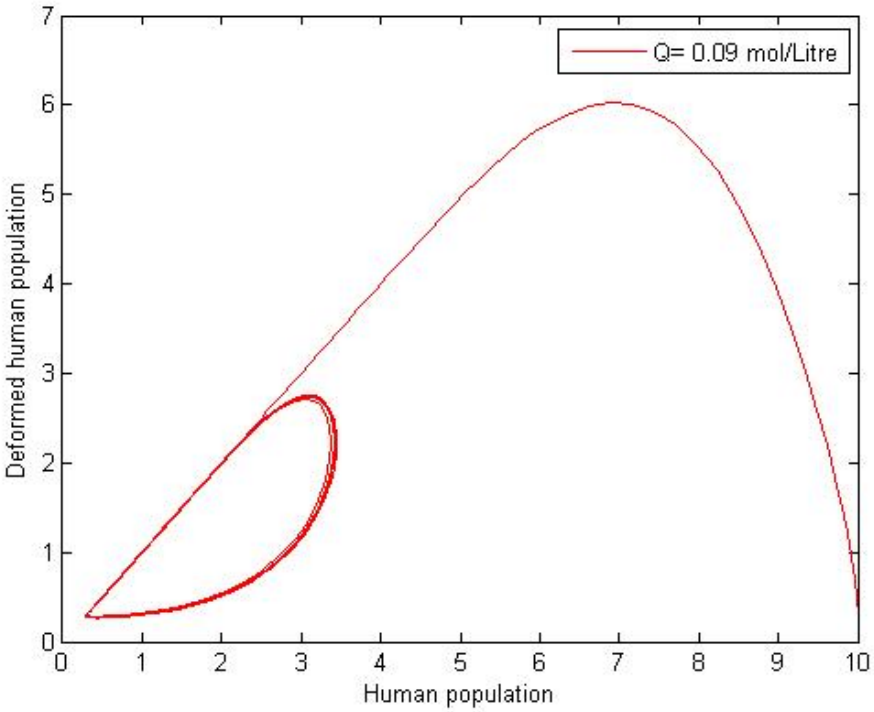
Q= 0.09 mol/Litre
Deformed human population
Human population
0
1
2
3
4
5
6
7
8
9
10

Figure 6:

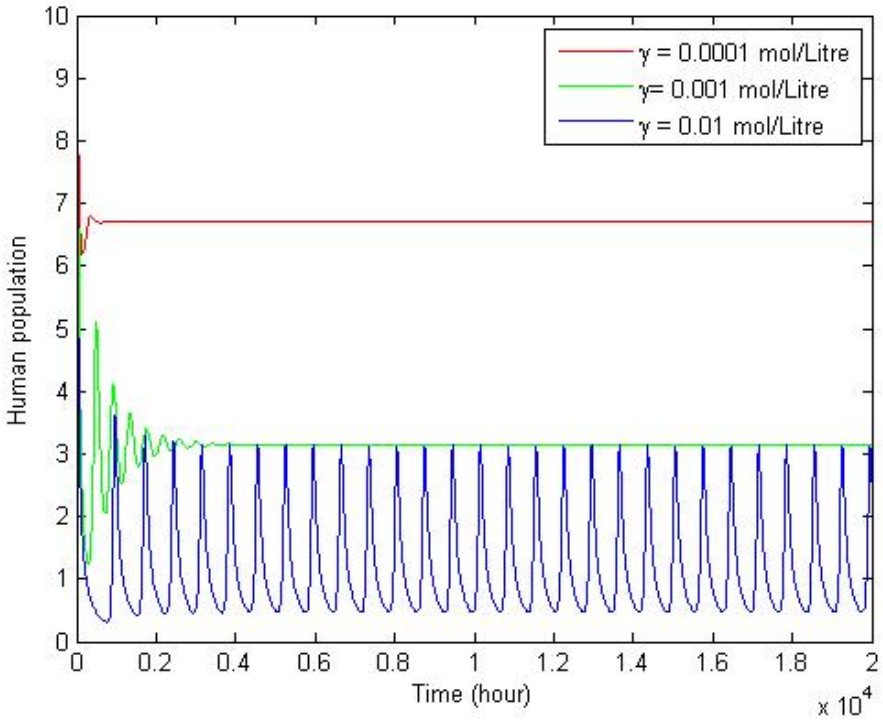
γ = 0.0001 mol/Litre
γ= 0.001 mol/Litre
γ = 0.01 mol/Litre
Human population
Time (hour)
x 10^4
0
1
2
3
4
5
6
7
8
9
10
0.2
0.4
0.6
0.8
1.2
1.4
1.6
1.8

Figure 7:

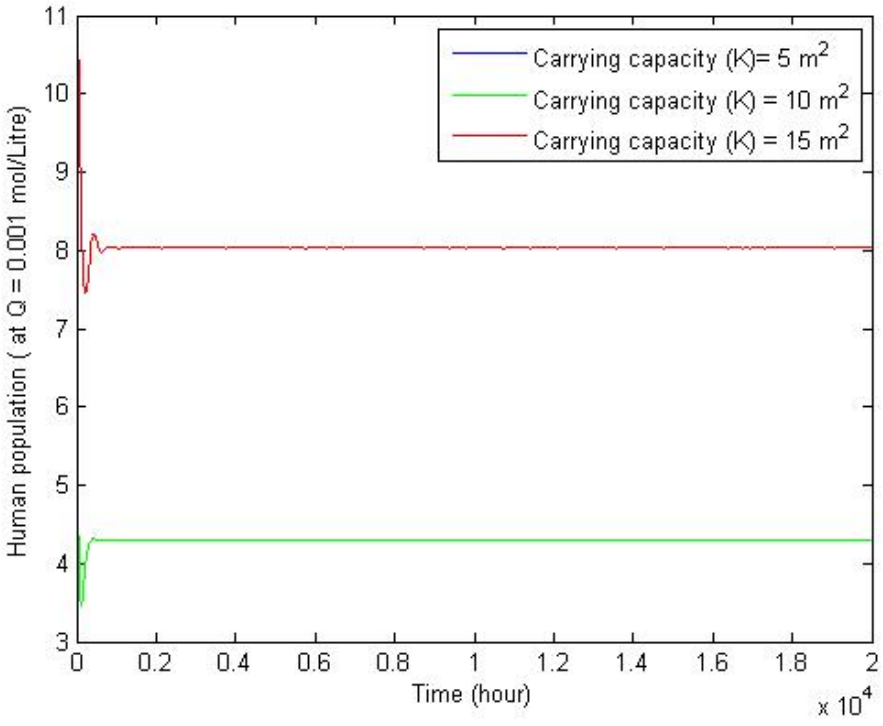
Carrying capacity (K)= 5 m2
Carrying capacity (K) = 10 m2
Carrying capacity (K) = 15 m2
Human population (at Q = 0.001 mol/Litre)
Time (hour)
x 10^4
11
10
9
8
7
6
5
4
3
0
0.2
0.4
0.6
0.8
1
1.2
1.4
1.6
1.8
2

Figure 8:

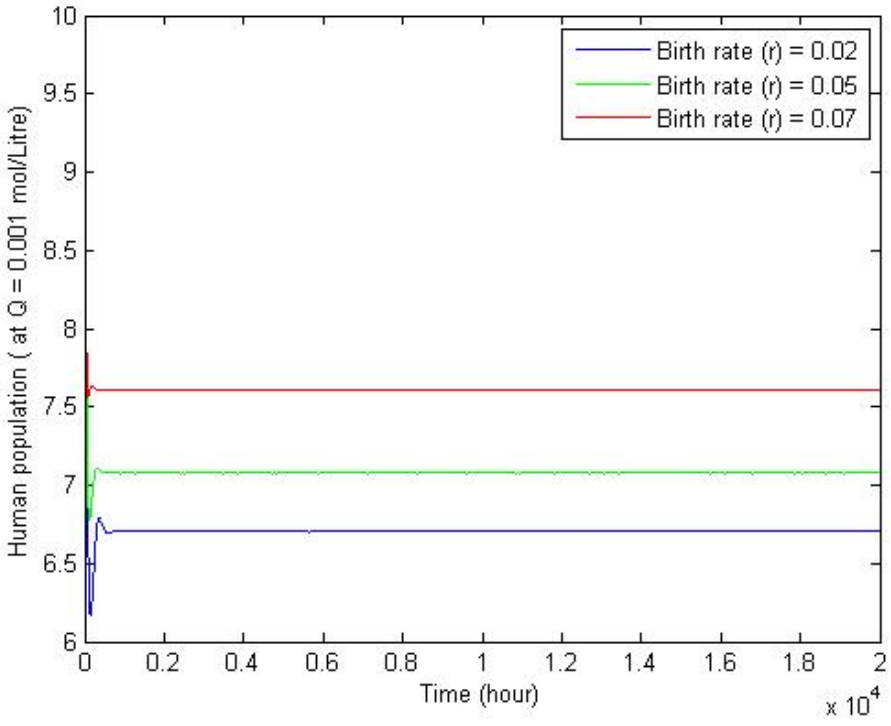
Birth rate (r) = 0.02
Birth rate (r) = 0.05
Birth rate (r) = 0.07
Human population (at Q = 0.001 mol/Litre)
Time (hour)
x 10^4
10
9.5
9
8.5
8
7.5
7
6.5
6
0
0.2
0.4
0.6
0.8
1
1.2
1.4
1.6
1.8
2

Figure 9:

density (P) decreases, while the density of the deformed population (P_D) initially rises before declining. Once Q exceeds the critical value, both densities exhibit oscillatory behavior, resulting in a supercritical Hopf bifurcation with stable periodic solutions (see Figs. 6, 7).

It is well established that pollutants released by human activities–such as industrial waste, vehicle emissions, and radioactive materials–contain toxic substances harmful to all living populations, including humans. While humans may not experience direct morphological deformities, exposure to these toxicants significantly affects health, leading to conditions such as bronchial asthma, lung cancer, chronic obstructive pulmonary disease (COPD), and reduced reproductive capacity. Consequently, the mortality rate among affected individuals increases.

The fuzzy set plays a very important role in terms of data uncertainties in this type of model. It is difficult to get real data for all the model parameters. However, selection of such parameters' values within their bound enable the identification of the toxicant emission rate threshold.

6 Conclusion

This study presents a nonlinear mathematical model to investigate the effects of a toxicant on human health, particularly on individuals who experience severe toxicity-induced reproductive impairment. The model assumes that the human population itself emits the toxicant into the environment. The system exhibits four equilibrium points: $E_0 = (0, 0, 0, 0)$, $E_1 = (K_0, 0, 0, 0)$, $E^* = (P^*, P*_D, C*, U*)$, and $E^{**} = (P^{**}, P**_D, C**, U**)$. The first equilibrium point i.e. E_0 is a saddle point. The second equilibrium point i.e. E_1 is stable under certain conditions, which means that the human population would settle down to its equilibrium level. The third and the fourth equilibrium points i.e. E^* and E^{**} are unstable due to toxicant accumulation in the human environment.

Funding

Not applicable

Availability of data and materials

The data used in this work are properly cited.

Code availability

The codes used in this work will be made available on request from the corresponding author.

References

[1] Trumble, B. C., & Finch, C. E. (2019). The exposome in human evolution: From dust to diesel. *Quarterly Review of Biology, 94*(4), 333–394. https://doi.org/10.1086/706768

[2] Tapia, J., Murray, J., Ormachea, M., Tirado, N., & Nordstrom, D. K. (2019). Origin, distribution, and geochemistry of arsenic in the Altiplano-Puna Plateau of Argentina, Bolivia, Chile, and Perú. *Science of the Total Environment, 678*, 309–325. https://doi.org/10.1016/j.scitotenv.2019.04.084

[3] Crews, D., & Gore, A. C. (2012). Epigenetic synthesis: A need for a new paradigm for evolution in a contaminated world. *F1000 Biology Reports, 4*, 18.

[4] Barrett, R., & Schluter, D. (2008). Adaptation from standing genetic variation. *Trends in Ecology & Evolution, 23*(1), 38–44. https://doi.org/10.1016/j.tree.2007.09.008

[5] Martin, E. M., & Fry, R. C. (2018). Environmental influences on the epigenome: Exposure-associated DNA methylation in human populations. *Annual Review of Public Health, 39*, 309–333. https://doi.org/10.1146/annurev-publhealth-040617-014629

[6] Russo, G. L., Vastolo, V., Ciccarelli, M., Albano, L., Macchia, P. E., & Ungaro, P. (2017). Dietary polyphenols and chromatin remodeling. *Critical Reviews in Food Science and Nutrition, 57*(12), 2589–2599. https://doi.org/10.1080/10408398.2015.1062353

[7] Nettore, I. C., Franchini, F., Palatucci, G., Macchia, P. E., & Ungaro, P. (2021). Epigenetic mechanisms of endocrine-disrupting chemicals in obesity. *Biomedicines, 9*(11), 1716. https://doi.org/10.3390/biomedicines9111716

[8] Lieb, J. D., Beck, S., Bulyk, M. L., Farnham, P., Hattori, N., Henikoff, S., Liu, X. S., Okumura, K., Shiota, K., Ushijima, T., et al. (2006). Applying whole-genome studies of epigenetic regulation to study human disease. *Cytogenetic and Genome Research, 114*(1), 1–15. https://doi.org/10.1159/000091922

[9] Okano, M., Bell, D. W., Haber, D. A., & Li, E. (1999). DNA methyltransferases Dnmt3a and Dnmt3b are essential for de novo methylation and mammalian development. *Cell, 99*(3), 247–257. https://doi.org/10.1016/S0092-8674(00)81656-6

[10] Rao, R., & Leibler, S. (2022). Evolutionary dynamics, evolutionary forces, and robustness: A nonequilibrium statistical mechanics perspective. *Proceedings of the National Academy of Sciences, 119*(14), e2112083119. https://doi.org/10.1073/pnas.2112083119

[11] Zhang, Z., Ramstein, G., Schuster, M., Li, C., Contoux, C., & Yan, Q. (2014). Aridification of the Sahara Desert caused by Tethys Sea shrinkage during the Late Miocene. *Nature, 513*(7518), 401–404. https://doi.org/10.1038/nature13705

[12] Dupont, L. (2003). Reconstructing pathways of aeolian pollen transport to the marine sediments along the coastline of SW Africa. *Quaternary Science Reviews, 22*(2â4), 157–174. https://doi.org/10.1016/S0277-3791(02)00032-X

[13] Thakur, S. A., Hamilton, R. F., & Holian, A. (2008). Role of scavenger receptor A family in lung inflammation from exposure to environmental particles. *Journal of Immunotoxicology, 5*(2), 151–157. https://doi.org/10.1080/15476910802085863

[14] Novakowski, K. E., Yap, N. V. L., Yin, C., Sakamoto, K., Heit, B., Golding, G. B., & Bowdish, D. M. E. (2018). Human-specific mutations and positively selected sites in MARCO confer functional changes. *Molecular Biology and Evolution, 35*(2), 440–450. https://doi.org/10.1093/molbev/msx298

[15] Hamilton, R. F., Thakur, S. A., Mayfair, J. K., & Holian, A. (2006). MARCO mediates silica uptake and toxicity in alveolar macrophages from C57BL/6 mice. *Journal of Biological Chemistry, 281*(44), 34218–34226. https://doi.org/10.1074/jbc.M605229200

[16] Sun, W., Hong, Y., Li, T., Chu, H., Liu, J., & Feng, L. (2022). Application of sulfur-coated magnetic carbon nanotubes for extraction of some polycyclic aromatic hydrocarbons from water resources. *Chemosphere, 309*, 136632. https://doi.org/10.1016/j.chemosphere.2022.136632

[17] Liu, Y., Zhang, H., Zhang, H., Niu, Y., Fu, Y., Nie, J., Yang, A., Zhao, J., & Yang, J. (2018). Mediation effect of AhR expression between polycyclic aromatic hydrocarbons exposure and oxidative DNA damage among Chinese occupational workers. *Environmental Pollution, 243*, 972–977. https://doi.org/10.1016/j.envpol.2018.09.014

[18] Schlebusch, C. M., Gattepaille, L. M., Engström, K., Vahter, M., Jakobsson, M., & Broberg, K. (2015). Human adaptation to arsenic-rich environments. *Molecular Biology and Evolution, 32*(6), 1544–1555. https://doi.org/10.1093/molbev/msv046

[19] Schlebusch, C. M., Lewis, C. M., Vahter, M., Engstrm̈, K., Tito, R. Y., Obregón-Tito, A. J., Huerta, D., Polo, S. I., Medina, Á. C., Brutsaert, T. D., et al. (2013). Possible positive selection for an arsenic-protective haplotype in humans. *Environmental Health Perspectives, 121*(1), 53–58. https://doi.org/10.1289/ehp.1205504

[20] Fraga, M. F., Ballestar, E., Paz, M. F., Ropero, S., Setien, F., Ballestar, M. L., Heine-Suñer, D., Cigudosa, J. C., Urioste, M., Benitez, J., et al. (2005). Epigenetic differences arise during the lifetime of monozygotic twins. *Proceedings of the National Academy of Sciences of the United States of America, 102*(30), 10604–10609. https://doi.org/10.1073/pnas.0500398102

[21] Chen, C., Qi, H., Shen, Y., Pickrell, J., & Przeworski, M. (2017). Contrasting determinants of mutation rates in germline and soma. *Genetics, 207*(1), 255–267. https://doi.org/10.1534/genetics.117.1114

[22] Zhou, Y., He, F., Pu, W., Gu, X., Wang, J., & Su, Z. (2020). The impact of DNA methylation dynamics on the mutation rate during human germline development. *G3: Genes, Genomes, Genetics, 10*(10), 3337–3346. https://doi.org/10.1534/g3.120.401511

[23] Skinner, M. K. (2016). Epigenetic transgenerational inheritance. *Nature Reviews Endocrinology, 12*(2), 68–70. https://doi.org/10.1038/nrendo.2015.206

[24] Skinner, M. K., Guerrero-Bosagna, C., & Haque, M. M. (2015). Environmentally induced epigenetic transgenerational inheritance of sperm epimutations promote genetic mutations. *Epigenetics, 10*(8), 762–771. https://doi.org/10.1080/15592294.2015.1062207

[25] Leung, Y.-K., Ouyang, B., Niu, L., Xie, C., Ying, J., Medvedovic, M., Chen, A., Weihe, P., Valvi, D., Grandjean, P., et al. (2018). Identification of sex-specific DNA methylation changes driven by specific chemicals in cord blood in a Faroese birth cohort. *Epigenetics, 13*(3), 290–300.

[26] Yauk, C., Polyzos, A., Rowan-Carroll, A., Somers, C. M., Godschalk, R. W., Van Schooten, F. J., Berndt, M. L., Pogribny, I. P., Koturbash, I., Williams, A., et al. (2008). Germ-line mutations, DNA damage, and global hypermethylation in mice exposed to particulate air pollution in an urban/industrial location. *Proceedings of the National Academy of Sciences of the United States of America, 105*(2), 605–610. https://doi.org/10.1073/pnas.0705896105

[27] Schuller, A., Bellini, C., Jenkins, T., Eden, M., Matz, J., Oakes, J., & Montrose, L. (2021). Simulated wildfire smoke significantly alters sperm DNA methylation patterns in a murine model. *Toxics, 9*(9), 199. https://doi.org/10.3390/toxics9090199

[28] Cheng, Y., Tang, Q., Lu, Y., Li, M., Zhou, Y., Wu, P., Li, J., Pan, F., Han, X., Chen, M., et al. (2022). Semen quality and sperm DNA methylation in relation to long-term exposure to air pollution in fertile men: A cross-sectional study. *Environmental Pollution, 300*, 118994. https://doi.org/10.1016/j.envpol.2022.118994

[29] Zama, A. M., & Uzumcu, M. (2009). Fetal and neonatal exposure to the endocrine disruptor methoxychlor causes epigenetic alterations in adult ovarian genes. *Endocrinology, 150*(10), 4681–4691. https://doi.org/10.1210/en.2009-0499

[30] Achema, K. O., Okuonghae, D., & Tongo, I. (2021). Dual-level toxicity assessment of biodegradable pesticides to aquatic species. *Ecological Complexity, 45*, 100911. https://doi.org/10.1016/j.ecocom.2021.100911

[31] Kumar, A., Agrawal, A. K., Hasan, A. K., & Misra, A. K. (2016). Modeling the effect of toxicant on the deformity in a subclass of a biological species. *Modeling Earth Systems and Environment, 2*, 40. https://doi.org/10.1007/s40808-016-0086-x

[32] Barros, L. C. de, Ferreira Leite, M. B., & Bassanezi, R. C. (2003). The SI epidemiological models with a fuzzy transmission parameter. *Computers & Mathematics with Applications, 45*, 1619–1628. https://doi.org/10.1016/S0898-1221(03)00141-X

[33] Mickens, R. E. (2007). Numerical integration of population model satisfying laws: NSFD methods. *Journal of Biological Dynamics, 1*, 427–436. https://doi.org/10.1080/17513750701605598

[34] Verna, R., Tiwari, S., & Upadhyay, R. K. (2017). Dynamical behaviour of fuzzy SIR epidemic model. In *Proceedings of the Conference of the European Society for Fuzzy Logic and Technology* (pp. 482–492). https://doi.org/10.1007/978-3-319-66827-7_45